TB66

19th International Symposium of Ballistics, 7–11 May 2001, Interlaken, Switzerland

HYDROCODE MODELLING OF HIGH-VELOCITY JET PENETRATION INTO SAND

A.D. Resnyansky and A.E. Wildegger-Gaissmaier

Weapons Systems Division, Defence Science and Technology Organisation, PO Box 1500, Salisbury SA, 5108 Australia

The paper studies theoretically the process of jet penetration into sand. The process is associated with mine neutralisation using a shaped charge. The hydrocode analysis employs an advanced model taking the strain-rate effects in the material into account and a conventional model from the database of the commercial DYNA hydrocode. DSTO tests revealed a significant reduction of velocity of the jet propagating through sand. This may lower the chances of the mine being neutralised by the detonation of the charge. The present study demonstrates that the type of the stress state being developed ahead of the penetrator is of primary importance to the penetration process. Hydrocode analysis of the stress state enables us to conclude that the profiling of shape charge resulting in an enlargement of the jet cross dimensions would allow one to increase the energy transmitted through the sand.

INTRODUCTION

Anti-personnel landmines and anti-vehicle mines have been used in recent conflicts in Cambodia, Somalia and Bosnia. Besides being a threat to peacekeeping forces they also pose considerable on-going danger to the civilian population long after the end of a conflict. Therefore an effective, safe procedure applied in the field is required for neutralisation of the threat. A variety of methods [1] ranging from counter charges, mechanical clearance, line charges, open detonation, projectile attack, explosive ordnance, laser and pyrotechnic devices have been investigated for use in landmine clearance. All of the methods have limitations in various scenarios being it cost, time required for the procedure or being hazardous for the operator. The current study investigates the physics involved in using shaped charges to neutralise landmines and discusses some of the limitations of this method.

The burial depth for anti-personnel (AP) mines are in the order of 30 mm whereas the burial depth of anti-tank (AT) mines can be in the order of 200 mm. Removing the overburden for neutralisation is not an option since a number of mines come with anti-tempering devices. Additional problems can arise during the neutralisation procedure if booster

or fuze of the mine is not functional or they are filled with a low sensitivity High Explosive (HE) like cast TNT. This implies that sufficient energy to cause either detonation or deflagration of a mine is required to make sure no residual unconsumed explosive remains after the procedure. It has been shown that shaped charges (SC) can be used to neutralise mines. This however requires a high enough jet velocity to penetrate the soil and detonate/deflagrate the mines.

The present paper is analysing the sand jet penetration. Hydrocode modelling was used to gain a better understanding of the physics and helped in the interpretation of experimental results which where conducted previously [2]. The study showed the limitations of the shaped charge method applied to landmine neutralisation.

THE PROBLEM STATEMENT

Detailed experimental analysis of a standard 38-mm-shaped charge has been conducted in [3]. The analysis confirmed a significant velocity gradient along the jet at the standoff distance of two charge calibres (76 mm). The paper's results is that for the observable 50 mm part of the jet the jet tip could have an effective velocity of nearly 7 km/s whereas the jet tail has a velocity in the range from 1 up to 3 km/s. From the photo-instrumentation data [3] the jet diameter varies from 1.2 to 2–3 mm. Experimental technique for determining the jet tip in [2,3] is taken from the literature [4]. In the tests [2] a capacitor discharge occurred due to the jet penetration. The capacitor gauges are copper screens of approximately 0.3 mm thickness and they characterise the time of arrival of the jet tip. Therefore, they could measure the average velocity between destruction of two neighbouring gauges.

Table 1

Point #	Screens (mm)	Test 1 (km/s)	Test 2 (km/s)	Test 3 (km/s)	Average (km/s)
1	0-25	4.69	4.65	4.94	4.76
2	25-50	4.43	4.43	4.31	4.36
3	25-75	4.14	4.11	3.98	4.08
4	75-100	3.73	3.62	3.82	3.73

The velocity data [2] for a dry sand penetrated by the SC jet at the conditions stated above are summarised in Table 1 for the sand depths from 0 to 100 mm. The complete summary of the data for the velocity averaged over the series of three shots is drawn in Fig 1. The reference distance of penetration is referred to the position of the second gauge. For instance, the first point in Fig 1 corresponding to the penetration distance $h=25\ mm$ is the average velocity V_p calculated from the capacitor discharge signals for two screens at 0 and 25 mm.

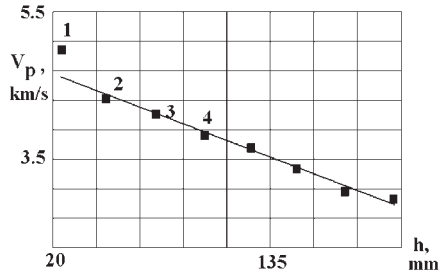

Figure 1. Results of the jet penetration test.

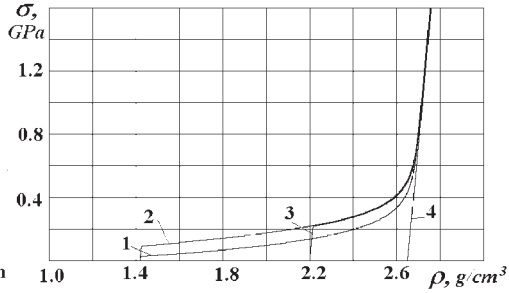

Figure2. Hugoniots calculated for the sand.

During interaction of the copper jet with sand a significant pressure might be developed in the sand. However small cross dimension of the jet results in a fast relaxation of the stress. Therefore, two stages of the jet penetration are of special interest to us. At the first stage the shock wave being developed is very important and might be a cause of the damage resulting in the gauge discharge. After the jet erosion and the lateral release of the shock due to insufficient confinement of the porous material the direct hit of the jet may prevail. These factors will be the subject of the present study.

MATERIAL MODELS

Two material models are employed in the paper. The advanced model [5] takes the strain rate effects of the sand into account. Constitutive relations combine two types of nonequilibrium of a porous material – shear stress relaxation and volumetric relaxation. In one-dimensional form the combination is expressed in the following form:

$$\frac{d\varepsilon_1}{dt}=\frac{\partial u}{\partial x}-\frac{\varepsilon_1-\varepsilon_2}{\tau_s}-\frac{\varepsilon_1+2\varepsilon_2}{\tau_v},\quad \frac{d\ln(\rho_*)}{dt}=-\frac{\varepsilon_1+2\varepsilon_2}{\tau_v},$$

here ρ_* is the material reference density which is related to the current volumetric porosity θ as $\rho_*/\rho_{00} = 1 - \theta$, ρ_{00} is the reference density of compacted material, $\varepsilon_1, \varepsilon_2$ – elastic deformations, and u – velocity. The relaxation functions τ_s and τ_v are fitted to the experimental Hugoniots and stress-strain data. To obtain a schematic of the sand response the experimental data [6] have been used for the fitting of τ_v. Corresponding Hugoniots for the sand are shown in Fig. 2 at different strain rates and initial porosity. Curves 1 and 2 correspond to initial density 1.42 g/cm^3 and strain rates 10 and 10^3 1/s, respectively. Curves 3 and 4 correspond to the strain rate 10^3 1/s and initial densities 2.2 and 2.65 g/cm^3. The curve 4 is the Hugoniot of the material in a solid phase.

The same material model is employed for the copper jet. The volumetric relaxation is neglected for this material. Material constants of the constitutive relation τ_s are fitted from the data of yield limit versus strain rate available in literature. The second model, which has been used in the commercial version of LS-Dyna3D [7], is a soil and foam material (material #5), the material constants have been fitted using the same experimental data. The advanced material model has been incorporated within LS-Dyna2D [8]. This version can operate only within the Lagrangian approach. Therefore, the Dyna2D calcu-

lations have been limited by moderate deformations. The model [5] has also been realised as a one-dimensional code for the cases of uniaxial strain and uniaxial stress.

HYDROCODE MODELLING

One-dimensional Analysis

In order to assess the influence of the stress state on the shock transmission properties the calculation of impact by a copper impactor on a sand target has been conducted in two statements: i) uniaxial strain, and ii) uniaxial stress. The first statement is correspondent to the plate impact test that is valid unless the lateral release reaches the shock propagating over sand. The uniaxial stress statement corresponds to the rod impact conditions where the lateral release is prevailing and cross (confinement) stresses are considered to be negligible.

Thickness of the impactor is chosen to be 50 mm, thickness of the target –75 mm ($x=x_t$ – position of the gauge at 75 mm). The process is analysed within the first 4 microseconds when the wave induced by the impactor is reaching the first point of interest (gauge) at 25 mm. The velocity distribution within the copper impactor is taken to be gradually decreasing from 7 km/s at the copper-target interface down to 3 km/s at the rear free surface $(x=x_r)$ of the impactor.

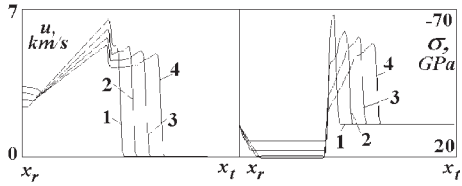

Figure 3. Calculation of the shock wave propagation in the sand at uniaxial strain.

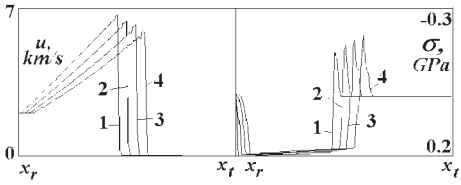

Figure 4. Calculation of the shock wave propagation in the sand at uniaxial stress.

The velocity- and stress-profiles for these two statements are calculated in the area $xr<x<xt$ and are drawn in Figs. 3 and 4, respectively. Four consecutive profiles 1–4 at 1, 2, 3, and 4 μsec, respectively, are drawn for each of the statements. In reality the impactor (SC jet) is not stretching so much because it is disintegrated into pieces which provide a tandem collision with the target. We ignore this detail concentrating on the pulse transmission through the sand. Comparing the figures it is seen that the lateral release plays a significant role for the transmission of pulse through sand. For the plate impact (Fig. 3) a slight velocity reduction is observed whereas the stress pulse transmitted is very high even though it is attenuating significantly. Obviously this stress would provide the pulse which is large enough to initiate detonation of high explosive behind the target. However, with the instantaneous release of the lateral stress (Fig. 4) the stress pulse transmitted is very low and comparable with the yield limit for copper. Despite of high kinetic energy of the head flow, the impactor delivers the major part of energy itself.

In order to assess the relative role of the stress regimes in the conditions which are closer to real ones a number of multi-dimensional calculations have been conducted.

Hydrocode Modelling with LS-DYNA2D

A two-dimensional Lagrangian calculation was conducted in a simplified statement with impact of a fragment (jet tip) of length in 10 mm having velocity 7 km/s over a sand target. The model described in previous section has been incorporated within LS-Dyna2D [8] and employed in the current calculation. Because of the limitation of the statement only the calculation up to the moment of the jet collision with the screen at 25 mm was considered. At later stages the slower parts of the jet plays an essential role but significant distortions of the grid make such a calculation difficult.

Fig. 5 (a–g) presents results of the calculation at several moments of time from 0 up to 6 μ*sec*, respectively. Figs. 5 (e–f) are complemented by contours of velocity, which are correspondent to the velocity module of approximately 2.5 km/s. This is a reference contour for comparison with calculations in the subsequent section. Taking symmetry into account only the positive side of the symmetry axis *(r>0)* is drawn. Parts of sand which are not effected by the projectile are deleted from the calculation in Figs. 5 (e–g).

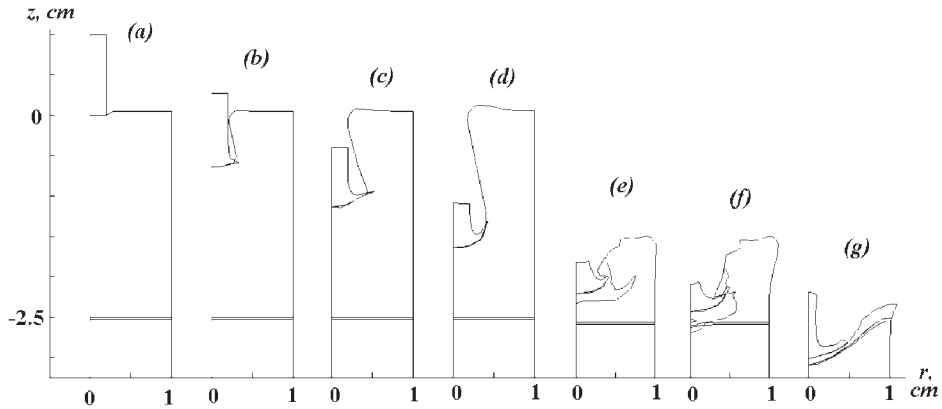

Figure 5. The 2D-hydrocode modelling of the jet penetration into sand with the advanced model.

Looking at the gauge/screen at 25 mm, the reference contour intersects the screen area at t=5 μ*sec*. The area of interaction of the projectile with sand is large enough to produce a significant pulse followed by the screen destruction which is broken soon after this instant.

In order to consider in details the whole set of factors effecting the problem Eulerian modelling with LS-DYNA3D has been conducted.

Eulerian Modelling

With the Eulerian approach the jet was represented as a continuous rod subdivided into 5 subsections of 10 mm in length. Each subsection has a constant velocity, which is 1 km/s less than the preceding subsection starting with 7 km/s for the head one.

Results of the simulation are shown in Figs. 6–8 depicting the target area. Screens at 25 and 75 mm are Lagrangian domains embedded into the Eulerian sand-projectile zone. We trace here only the contact interfaces between the projectile and sand along with the screens, which could be a subject of erosion. A certain concentration of mass close to 1 determines the level contour of the projectile-sand interface. For each of the contours an additional one depicting the velocity contour ahead of the projectile is drawn. The velocity level is the same as in Fig. 5. The drawings *(a–d)* are correspondent to the time moments at 4, 5, 11.75 and 18.75 μ*sek*, respectively. The mesh resolution in calculations of Figs. 6 and 8 is in agreement with that in Fig. 5. The jet tip diameter is smaller in Fig. 6 than that in Fig. 5. The Eulerian mass diffusion of the projectile is significant in the case of Fig. 6. This might be a reason of reduced resistance of the sand material and closer position of the shock to projectile.

Figure 6. Eulerian calculation on a standard mesh.

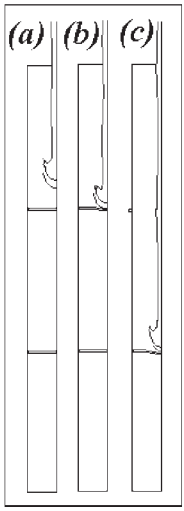

Figure 7. Calculation of the thin jet propagation.

Figure 8. Calculation on a refined mesh.

To study the shape resistance a calculation with half the initial diameter of the projectile has been conducted (Fig. 7). This result confirms that jet velocity is approximately the same and the shock effect is reduced. To reduce the Eulerian erosion effects the calculation of Fig. 6 has been repeated with a finer mesh size (2 times) in the radial direction (Fig. 8). It is seen that the jet tip area in this case is comparable with that of the Lagrangian calculation (Fig. 5). Due to the increase of the cross-sectional area of the jet tip the shock affect in the case of Fig. 8 is slightly higher than that for Fig. 6. However, it is still lower than that in Fig. 5. This can be attributed to quasi-static material properties of the current model.

DISCUSSION

The hydrocode simulations have shown reasonable agreement with experiment employing the current material models and the problem statements. The study proved that the first point (point 1 in Fig. 1) is a result of gauge destruction by the shock wave induced by the SC jet. The rest of the data are likely to be caused by the direct collision of the jet with gauges. Thus, the actual velocity of the jet is slightly lower and very close to the straight line passing through the rest of the points (line in Fig. 1).

The model has also demonstrated that the transition from the plate impact regime to the rod penetration regime effects significantly the shock transmission into sand. The shock transmission is of benefit to the landmine clearance process. Concluding, the energy could be provided underground by two ways: energy of the shock wave or direct energy of collision of the jet. For the direct hit by jet a significant mass intake is not easy to provide because of significant erosion of the material in soil. On the other hand, the confinement is not strong enough in soils in order to support the shock in the ground from a compact impactor. An alternative could be an increase of the effective area of interaction of the impactor with soil (profiling SC in order to increase the jet diameter) or arranging a shock wave close to the plane one. In spite of the fact that the velocity of the projectile might be reduced with such an arrangement chances to gain higher pressure at the buried mine and, hence, to induce its detonation could be higher.

REFERENCES

1. R. Bird, "Landmine Neutralisation", *Land Warfare Conference*, Melbourne, Australia, Oct. 2000
2. R. Bird, "Landmine Clearance Using a Shaped Charge Device", *3rd Meeting of the TTCP AG "Mines Disposal Technologies (Land)"*, DSTO-Salisbury, Adelaide, Australia 10–14 April 2000
3. M.Chick and G.P.Briggs, "Fabrication and Performance Assessment of Shaped Charges", *Defence Standards Laboratories report 546*, Melbourne, Australia, 1974
4. R.J.Eichelberger, *J of Applied Physics 26*, 398, 1955
5. E.I. Romenskii, "Relaxation Model for Describing the Strain of Porous Materials", *J. of Appl. Mech. and Techn. Physics (transl. from Zh. Prikl. Mekh. Tekh. Fiz.) no. 5*, 145–149, 1988
6. T. Ando, H. Yamaguchi, M. Ui, T. Hoshikawa and K. Fujimoto, "A Study on the Impact Response of Buried Structures by Using the Centrifuge Test", *J. of Structural Engineering, 43A, JSCE*, 1469–1480, 1997
7. J.O. Hallquist, D.W. Stillman, and T.-L. Lin, *"LS-DYNA3D User's Manual,"* Livermore Software Technology Corporation, 1994
8. J.O. Hallquist, User's manual for DYNA2D – *An explicit two-dimensional hydrodynamic finite-element code with interactive rezoning*, Lawrence Livermore National Laboratory, UCID-18756, Rev. 2, 1984